EVIDENCE FOR COLD, HYDROUS PARENTAL MAGMAS ON DOMINICA: PETROLOGY OF THE FOUNDLAND BASALTS

KATHRYN VONSYDOW, California State University San Bernardino
Research Advisors: Laura Waters (Sedona College), Holli Frey (Union College), and Joan E. Fryxell (California State University San Bernardino)

INTRODUCTION TO RESEARCH QUESTION

Dominica is the center island of the Lesser Antilles island arc. The island hosts a variety of volcanic features that all contribute to the story of its formation. The Foundland (FND) region is in the southeastern portion of Dominica. FND is one of the few locations on the island where basalt has been erupted. The petrology of the basalts and their field relations in FND will contribute to an understanding of the primitive magmas that formed under Dominica. These findings can then be compared to the data collected from another basalt location, proto-Morne aux Diables (pMAD), in the northern section of the island which is thought to have erupted around the same time to determine if they originated from the same magmatic source.

GEOLOGIC BACKGROUND

FND is in the southeast corner of Dominica and is thought to represent one of the most primitive magmas erupted on the island. One notable feature of this region is the absence of felsic deposits and the eruption of basalts. The basalts of the FND stratovolcano are thought to have erupted 3.72 to 1.12 mya during the Pliocene Epoch (Smith et al., 2013). The oldest rocks of FND can be found along the base of sea cliffs and are volcanic breccia deposits (Wills, 1974). The inland regions of FND are dominated by up to 30 m thick basalt flows interbedded with scoriaceous pyroclastic deposits and some andesites (Lindsay et al., 2005).

METHODS

One major obstacle of fieldwork was finding locations to collect viable rock samples. Wills (1974) gave the GPS coordinates of locations of his sample sites around FND. Due to road damage from Tropical Storm Erika that hit the island in 2015, it was very difficult to reach the interior portion of FND. We were only able to collect samples from Foundland's easternmost and westernmost edges. Samples were collected from outcrops exposed along roadcuts and river floodplains using 6-pound and 10-pound sledgehammers.

At Union College, the best pieces were selected from each sample and were cut to the proper dimensions for 11 thin sections using a diamond tipped rock saw. The resulting billets were epoxied, cut, and polished in the Geology Department at Union College. Three of the thin sections were given a carbon coat and examined under a scanning electron microscope (SEM) along with a sample previously collected by Frey (Foundland-2B). Images and compositions of spinel (mostly magnetite), olivine, and plagioclase were collected using energy dispersive spectrometry (EDS) with the Zeiss EVO-MA15 Scanning Electron Microscope (SEM) at Union College. The EDS analyses were conducted following a calibration method, where the initial beam intensity is obtained by collecting the energy emitted by a copper plate, then EDS spectra are collected for natural mineral standards in the Union College collection.

Using a Rocklabs hydraulic press provided by Union College, samples were crushed into rock fragments and then dried in an oven before being broken down into smaller fragments with a small sledgehammer.

Table 1. Bulk chemistry of Foundland samples

Sample Number	FB-1A	FB-2A	FB-2M	FB-3	FB-4	FB-5	FB-6	FB-7A	FB-7B	FB-8	FB-9
Major Elements, in weight percent											
SiO2	52.74	52.54	48.74	52.10	51.67	59.32	51.51	48.79	48.81	49.37	52.95
TiO2	0.83	0.81	1.06	0.86	0.90	0.69	0.82	0.97	1.05	1.02	0.83
Al2O3	19.36	19.72	19.82	20.80	20.27	17.94	21.41	21.18	21.01	20.40	19.93
Fe2O3	9.74	9.20	11.39	8.84	9.52	7.75	8.94	9.89	10.30	10.67	9.17
MnO	0.20	0.19	0.20	0.19	0.19	0.14	0.19	0.17	0.18	0.19	0.20
MgO	4.50	4.59	5.52	3.81	4.14	2.74	3.70	5.38	4.83	5.10	4.08
CaO	9.07	9.53	10.70	9.93	10.11	7.07	10.32	10.77	10.94	10.44	9.55
Na2O	2.75	2.64	2.09	2.58	2.49	2.78	2.32	2.14	2.08	2.19	2.51
K2O	0.54	0.51	0.26	0.61	0.47	1.34	0.53	0.49	0.53	0.39	0.54
P2O5	0.15	0.14	0.08	0.14	0.12	0.10	0.12	0.11	0.11	0.09	0.13
Total	99.87	99.87	99.84	99.87	99.86	99.87	99.88	99.88	99.84	99.87	99.88
Trace Elements, in parts per million											
Rb											
Sr	11	11	4	14	9	44	11	14	15	5	16
Ba	295	294	278	284	348	226	271	240	294	234	235
Zr	117	108	106	129	105	231	105	123	153	93	118
Y	53	51	37	64	45	79	57	21	51	48	57
Nb	21	18	15	19	17	24	18	0	17	20	22
Cs	0	3	4	4	0	5	4	0	7	0	7
Sc	0	0	0	0	7	0	0	0	0	0	7
V	28	30	45	28	32	24	23	49	34	37	25
Cr	221	226	389	237	255	191	220	354	365	344	221
Ni	15	19	11	7	13	7	10	0	3	19	14
Cu	10	11	10	8	11	3	8	0	13	10	8
Zn	52	78	129	83	76	55	79	46	121	66	37
Ga	79	77	77	77	70	61	75	47	76	69	76
La	20	19	19	21	19	19	20	14	19	19	20
Ce	10	9	11	0	10	19	8	0	18	12	8
Nd	21	16	27	26	23	32	20	20	29	12	20
Hf	12	11	22	21	13	18	17	0	22	5	12
Pb	6	2	2	0	2	0	6	5	0	6	4
Th	4	4	3	5	6	5	4	0	9	6	3
U	0	0	3	0	0	4	0	8	2	0	0

The fragments were then placed inside a Rocklabs shatter box with aluminum oxide vessel and porcelain plate and ground into a fine powder. A powder was made from each sample (11 in total).

We determined major and trace element abundances using a 3.0 kW Panalytical Axios wavelength-dispersive X-ray fluorescence (XRF) spectrometer at Pomona College. Each of the 11 powders were prepared for analysis by mixing them with a flux in a 2:1 ratio (3.5 g basalt powder to 7.0 g dilithium tetraborate (Li2B4O7)). A vortex blender was then used to ensure the mixture was homogeneous. Each mixture was placed in a graphite crucible and fused into a glass bead at 1000 °C for 15 minutes, left to cool to room temperature, and reheated for an additional 15 minutes at 1000 °C to burn off any extra water still present, as well as eliminate any air pockets within the bead. The cooled beads where then polished on diamond polishing wheels and by hand with 400-grit sandpaper. Using XRF equipment provided by the Pomona College Geology Laboratory, we were able to analyze major, minor, and 22 trace elements

from each bead (Table 1). Reference calibration curves were defined by using 55 certified reference materials (Lackey et al., 2012).

Modal counts were collected for 1000 points each on four slides at Union College using a Petrog point count stage, the PetrogLite computer program, and a petrographic microscope. The modal counts of the remaining slides (excluding sample FB-5 which was determined to be an andesite) were collected for 1000 points each by hand using a petrographic microscope at CSUSB.

RESULTS

Major and Minor Elements

Table 1 shows major and trace element data for the FND samples. For the major elements, the silica content averaged 51.69 wt. % for each sample (except FB-5) and is classified as a basalt. The average Al2O3 content was 20.17 wt. % which can be an indicator that the parental melt experienced fractional crystal-
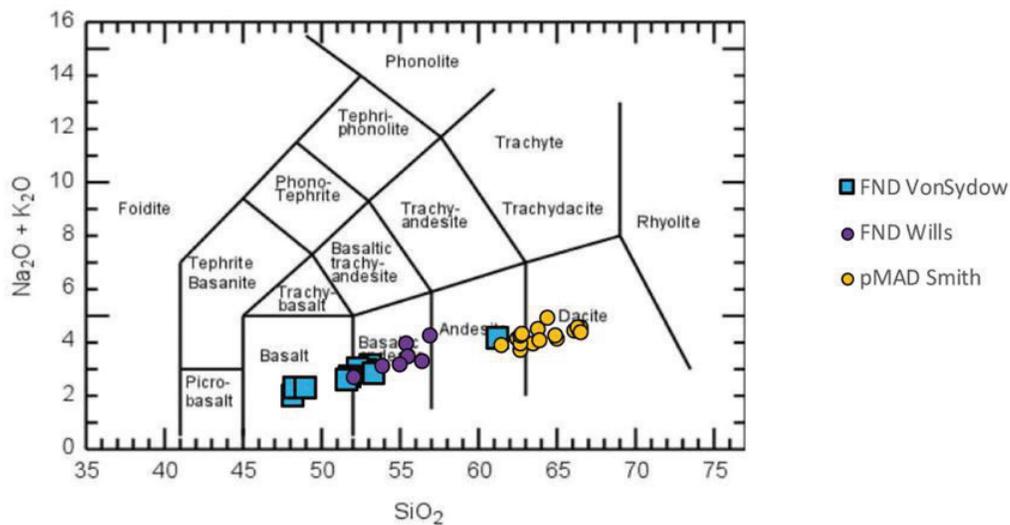
Figure 1. TAS Diagram (modified from LeBas et al., 1986) showing the relationship between SiO_2 content vs Alkali content of samples collected from FND and pMAD.

lization. For the minor elements, the average amount of TiO_2 was 0.89 wt. % and the average MnO was 0.18 wt.% which suggests the influence of oxidizing conditions. Sample FB-2M, a boulder that was collected in the Savanna River floodplain and contained mafic nodules, had the highest concentrations of TiO_2, Fe_2O_3, MnO, and MgO, which further supports oxidizing conditions. Alkali concentrations ($Na_2O + K_2O$) vs silica concentrations are plotted on Figure 1 and shows that the samples range from a basalt to basalt-andesite composition; however, Sample FB-5 was found to be an andesite.

Modal Abundances

Modal abundances, excluding sample FB-5, were determined from samples collected in FND. For each sample, plagioclase was the most frequently observed phenocryst, composing between 21.1 and 47.6%. Clinopyroxene (cpx) was the second most common phenocryst found in each sample constituting between 4% and 13.6%. Most olivine (olv) crystals were highly weathered and difficult to recognize; those that were observed composed between 1.1% and 8.7%. The abundance of orthopyroxene (opx) phenocrysts ranged between 1.1% and 3.2%. In most samples, groundmass (gm) was a major component of the rock and ranged between 25.1% and 62.3%.

Plagioclase Compositions

From the same four samples, the rim and core from five different phenocrysts each were analyzed using a SEM at Union College. We were unable to collect data from the rim of the second phenocryst in sample FB-2B. The composition of plagioclase rims ranged between An_{54} and An_{97} and the composition of cores ranged between An_{78} and An_{95}.

Olivine Compositions

Olivine compositions were established from rims and cores of phenocrysts from four samples. It was difficult finding unweathered olivine phenocrysts to analyze from each sample. Of those that were found, sample FB-2 has an average composition of Fo_{69}, FB-7A has an average composition of Fo_{70}, and FB-9 is the most forsteritic with an average composition of Fo_{78}.

Fe-Ti Oxide Compositions

Iron-titanium oxide composition were also determined from four samples. Fe-Ti oxide compositions fall on the titanomagnetite-ulvospinel continuum with trace amounts of the spinel end member. Higher oxygen environments cause ulvospinel components of magnetite to chemically weather by oxidation to form ilmenite.

Relatively high concentrations of Ti can only occur in low-oxidation environments; therefore, the low TiO_2 concentrations coupled with presence of ilmenite support the hypothesis that these samples formed under oxidizing conditions. Furthermore, the existence of both magnetite and ilmenite in samples (i.e. FB-2M and FB-9) require that the parental melt be subjected to a limited range of temperatures. Using an Fe-Ti oxide geothermobarometer created by Ghiorso and Evans (2008), we used all possible pairs to determine a temperature range as low as 714 °C and as high as 925 °C with an average of temperature around 816 °C.

Amphibole Phenocrysts

Amphibole phenocrysts were analyzed in sample FB-9 and fall on the cummingtonite-grunerite solid series; they also all contain trace amounts of calcium. Amphiboles appear late in the crystallization sequence associated with mafic rocks, specifically if the melt is enriched in silica and H_2O. The oxidized rims had formed around the phenocrysts indicating they grew from the melt and were not plucked a cumulate or country rock.

DISCUSSION

FND and pMAD are volcanic centers located at opposite ends of Dominica. Both centers erupted around the same time (Pliocene Epoch) and one outstanding question in the literature is whether they erupted from the same magma source (Smith et al., 2013). We note the presence of the same mineral phases (plagioclase + clinopyroxene + titanomagnetite ± ilmenite ± olivine ± orthopyroxene) in lavas erupting from both volcanic centers, however it is still outstanding if their major element patterns are both similar and consistent with the observed mineral phases.

FND samples are plotted along with those collected by Smith et al. (2013) and Wills (1974) for both FND and pMAD in Figure 2. Despite being relatively mafic samples, each suite of volcanics has a low concentration of MgO with markedly elevated alkali concentrations. The most striking pattern of all the FND and pMAD lavas is that all samples are saturated in abundant plagioclase crystals; this modality is largely consistent with elevated Al_2O_3 contents for each sample, which should stabilize plagioclase. The trends of

Al_2O_3 and CaO for all the lavas are consistent with the crystallization of plagioclase through a liquid line of descent. Additionally, the pattern of continuous depletion in Fe_2O_3 and TiO_2 throughout both volcanic series is consistent with the presence of magnetite-ulvospinel in all samples. The similar patterns in geochemistry for each of these areas suggests that they are derived from a similar source.

The most notable difference between both volcanic centers is the presence of amphiboles collected in FND (FB-9) and their absence in pMAD (Smith et al., 2013). This may be explained by both the water content and the pre-eruptive temperature of the melt during the two eruptive episodes. The phase stability curves for plagioclase and amphibole determined from experiments on high-Al basalt from Grove et al. (2003), demonstrate that the co-existence of plagioclase and amphibole only occurs at relatively cold pre-eruptive temperatures for a basalt (1000 °C – 1050 °C). Moreover, saturation in plagioclase and amphibole additionally requires between 7 – 8 wt. % H_2O to be in equilibrium with the melt (under pure H_2O vapor saturated conditions) (Fig. 3). One possible explanation for the presence of amphibole in the FND lavas is that they separated from their parental cumulates at lower temperatures. Additionally, Ca-rich plagioclase was observed in both FND and pMAD. In pMAD, phenocryst compositions covered a narrow range and were more anorthite-rich than FND, suggesting that pMAD's melt was in the earlier stages of crystallization (i.e. hotter) at the time of eruption.

With respect to mantle source, sample geochemistry and petrology reported in this study and from Smith et al. (2013) indicated that both the FND and the pMAD magmas were likely derived from a parental magma that originated from a metasomatized mantle. The calcic nature of the plagioclase crystals and the presence of amphibole in one sample from FND in all samples strongly supports high water contents. The discrepancy (i.e. differentiation) beneath FND occurs at lower temperatures, which suggests an interval of cooling occurred between the eruption of pMAD and FND.
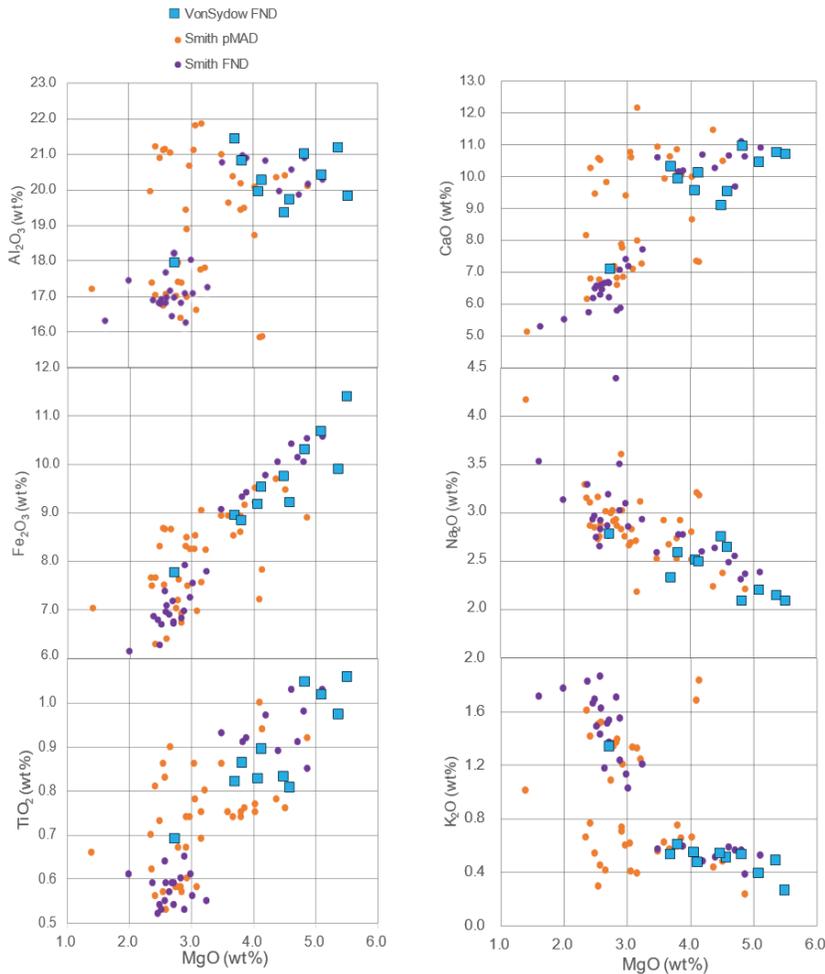
Figure 2. Harker diagrams showing the relationship between MgO concentration and major/minor element concentrations from FND and pMAD (Wills, 1974 and Smith et al., 2013).
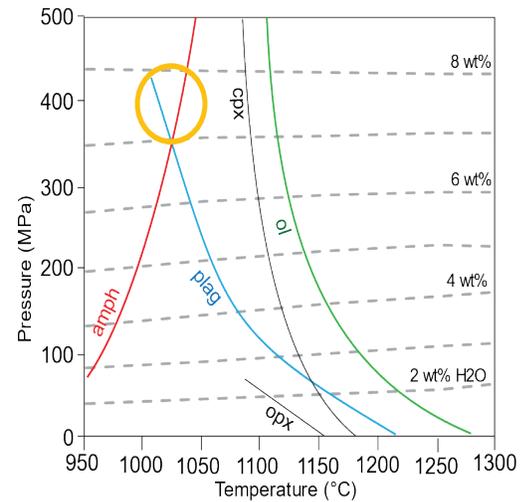

Figure 3. Results of a H₂O saturated phase equilibrium experiments modified from Grove et al. (2003). Amphibole (amph), plagioclase (plag), clinopyroxene (cpx), orthopyroxene (opx), and olivine (olv) lines are plotted to show the conditions necessary for their growth from a melt. The area circled in yellow suggests the conditions necessary for plagioclase and amphibole to coexist.

CONCLUSION

The overall bulk chemistry of samples collected from FND and pMAD show very similar trends. Both locations are characterized by the same mineral phases, highly calcic plagioclase, little to no olivine, and Fe-Ti oxides. The overall mineral composition of the samples from FND indicate they are aluminous, subduction zone basalts. When these basalts are compared to those collected in pMAD (Smith et al., 2013), we see that the compositions are very similar which suggests both locations shared the same magma source. The main difference between the two centers is the presence of amphibole phenocrysts in FND. The presence of amphibole crystals and the coexistence of magnetite and ilmenite, suggest that between the eruption of pMAD and the eruption of FND, the melt cooled and crystallized, explains the inferred increase in water and lower inferred temperature.

FURTHER STUDY

• Olivine phenocrysts collected from pMAD need to be analyzed to be compared to those collected in FND.

• More SEM work to be done on samples collected in FND to add to the data set.

ACKNOWLEDGEMENTS

REFERENCES CITED

Frey, H.M., Dominica: The Sleeping Giant in the Caribbean: Franklin and Marshall Magazine Issue 84, 52 p.

Ghiorso, M.S. and Evans, B.W., 2008, Thermodynamics of Rhombohedral Oxide Solid Solutions and a Revision of the Fe-Ti Two-oxide Geothermometer and Oxygen-barometer: American Journal of Science, v. 208, p. 957 – 1039.

Grove, T.L., Elkins-Tanton, L.T., Parman, S.W., Chatterjee, N., Müntener, O., and Gaetani, G.A., 2003, Fractional crystallization and mantle-melting controls on calc-alkaline differentiation trends: Contributions to Mineralogy and Petrology, v. 145, doi: 10.1007/s00410-003-0448-z.

Lackey, J.S., Cecil, M.R., Windham, C.J., Frazer, R.E., Bindeman, I.N., and Gehrels, G.E., 2012, Fine Gold Intrusive Suite: The roles of basement terranes and magma source development in the Early Cretaceous Sierra Nevada batholith: Geosphere, v. 8, no. 2, doi: 10.1130/GES00745.1.

LeBas, M.J., LeMaitre, R.W., Streckeisen, A., and Zanettin, B., 1985, A Chemical Classification of Volcanic Rocks Based on the Total Alkali-Silica Diagram: Journal of Petrology, v. 27, no. 3, p. 745 – 750.

Lindsay, J.M., Smith, A.L., Roobol, M.J., and Stasiuk, M.V., 2005, Volcanic Hazard Atlas of the Lesser Antilles: Dominica: West Indies, Seismic Research Centre, 279 p.

MacDonald, R., Hawkesworth, C.J., and Heath, E., 1999, The Lesser Antilles Volcanic Chain: A Study in Arc Magmatism: Earth-Science Reviews, v. 49, p. 1-76.

Smith, A.L., Roobol, M.J., Mattioli, G.S. Fryxell, J.E., Daly, G.E., and Fernandez, L.A., 2013, The Volcanic Geology of the Mid-Arc Island of Dominica, Lesser Antilles: The Surface Expression of an Island-Arc Batholith: Boulder, Colorado, Geological Society of America Special Paper 496, 249 p.

Wills, K.J.A., 1974, The geologic history of Southern Dominica and plutonic nodules from the lesser Antilles [Doctoral thesis]: Durham University, 211 p.